Molecular Basis of Cell and Developmental Biology:

In Vivo Regulation of Acetylcholinesterase Insertion at the Neuromuscular Junction

Isabel Martinez-Pena y Valenzuela, Richard I. Hume, Eric Krejci and Mohammed Akaaboune

J. Biol. Chem. 2005, 280:31801-31808.
doi: 10.1074/jbc.M502874200 originally published online July 5, 2005

THE JOURNAL OF BIOLOGICAL CHEMISTRY
Vol. 280, No. 36, Issue of September 9, pp. 31801–31808, 2005
Printed in U.S.A.

In Vivo Regulation of Acetylcholinesterase Insertion at the Neuromuscular Junction*

Received for publication, March 16, 2005, and in revised form, June 30, 2005
Published, JBC Papers in Press, July 5, 2005, DOI 10.1074/jbc.M502874200

Isabel Martinez-Pena y Valenzuela‡, Richard I. Hume‡, Eric Krejci§, and Mohammed Akaaboune‡¶

From the ‡Department of Molecular, Cellular and Developmental Biology, University of Michigan, Ann Arbor, Michigan 48109 and §INSERM U686, Biologie des Jonctions Neuromusculaires, UFR Biomédicale Paris 5, 45 Rue des Saints-Pères, 75006 Paris, France

The efficiency of synaptic transmission between nerve and muscle depends on the number and density of acetylcholinesterase molecules (AChE) at the neuromuscular junction. However, little is known about the way this density is maintained and regulated *in vivo*. By using time lapse and quantitative fluorescence imaging assays in living mice, we demonstrated that insertion of new AChEs occurs within hours of saturating pre-existing AChEs with fasciculin2, a snake toxin that selectively labels AChE. In the absence of muscle postsynaptic activity or evoked nerve presynaptic neurotransmitter release, AChE insertion was decreased significantly, whereas direct stimulation of the muscle completely restored AChE insertion to control levels. This activity-dependent AChE insertion is mediated by intracellular calcium. In muscle stimulated in the presence of a Ca^{2+} channel blocker or calcium-permeable Ca^{2+} chelator, AChE insertion into synapses was significantly decreased, whereas ryanodine or ionophore A12387 treatment of blocked and unstimulated synapses significantly increased AChE insertion. These results demonstrated that synaptic activity is critical for AChE insertion and indicated that a rise in intracellular calcium either through voltage-gated calcium channels or from intracellular stores is critical for proper AChE insertion into the adult synapse.

The maintenance of a high density of postsynaptic neurotransmitter receptors and transmitter inactivation molecules at the site of synaptic contact is critical for the functioning nervous system. In cholinergic synapses, acetylcholinesterase (AChE)[1] plays a critical role in the control of acetylcholine hydrolysis during synaptic transmission (1, 2). The efficacy by which AChE controls neurotransmitter lifetime in the synaptic cleft depends not only on its enzymatic activity but also on its density and location relative to acetylcholine receptors (AChRs). Although progress has been made in elucidating the cellular and molecular events regulating AChR dynamics at the postsynaptic membrane (3, 4), our knowledge concerning the cellular basis of AChE dynamics is relatively limited. In particular it is unclear how this molecule is inserted and maintained at the synapse *in vivo*. At the neuromuscular junction, AChE is organized in a tetramer by collagen Q (ColQ) and is tethered in the extracellular matrix via ColQ and a complex of associated proteins, including perlecan, dystroglycan, and a muscle-specific tyrosine kinase (5–7). Mutation or absence of ColQ or perlecan severely reduces the clustering of AChEs at neuromuscular junctions (NMJs) (8–10).

The availability of fasciculin2, a snake toxin purified from the green mamba *(Dendroaspis angusticeps*), and the presence of the large number of AChEs at the neuromuscular junction have enabled us to study directly the dynamics of AChE. Fasciculin2 belongs to the three-finger toxin family along with the well known acetylcholine receptor blocker, α-bungarotoxin (11), and has a high affinity for AChE (12–14). When fasciculin2 binds AChE, 94% of enzyme activity is inhibited, allowing only residual detectable AChE activity (15, 16). Previously, fasciculin2 has been used to characterize AChEs biochemically (11) as a probe to quantify AChE density in the mouse sternomastoid muscle (17), and fluorescently labeled fasciculin2 has been used to label AChEs on cultured cells, muscle cross-sections, and whole mounted muscle (18). In the present work, by saturating all pre-existing AChEs with unlabeled fasciculin2, we were able to monitor the subsequent insertion of new AChEs with fluorescently labeled fasciculin2. We found that AChEs were rapidly inserted into NMJs and that postsynaptic activity is necessary to enable normal AChE insertion through a mechanism mediated by intracellular calcium.

MATERIALS AND METHODS

Unless stated otherwise, compounds used in this study were obtained from Sigma. Unlabeled fasciculin2 (Latoxan, Valence France) and Alexa 594 fasciculin2 (conjugated by Molecular Probes Eugene, OR) were used to label AChE. Unlabeled and Alexa 488-conjugated bungarotoxin were obtained from Molecular Probes (Eugene, OR). To chelate cytosolic calcium, we used BAPTA-AM (Molecular Probes, Eugene, OR), a membrane-permeant substance that generates the high affinity calcium chelator BAPTA by the hydrolysis of ester bonds. As a control for any nonspecific effects of the hydrolysis products, we used Mag-Fura2-AM (Molecular Probes, Eugene, OR), which has a much lower affinity for calcium but generates the same by-products.

In Vivo Imaging of Neuromuscular Junctions—Non-Swiss Albino adult female mice (6–10 weeks old, 25–30 g) were obtained from Harlan Sprague-Dawley. The mice were anesthetized with an intraperitoneal injection of a mixture of ketamine and xylazine (17.38 mg/ml). Sternomastoid muscle exposure and neuromuscular junction imaging were done as described in detail previously (19–21). Briefly, the anesthetized mouse was placed on its back on the stage of a customized epifluores-

* This work was supported by the University of Michigan, NINDS Grant NS047332 from the National Institutes of Health (to M. A.), and National Science Foundation Grant IBN-0077634 (to R. I. H.). The costs of publication of this article were defrayed in part by the payment of page charges. This article must therefore be hereby marked "*advertisement*" in accordance with 18 U.S.C. Section 1734 solely to indicate this fact.

¶ To whom correspondence should be addressed: Dept. of Molecular, Cellular and Developmental Biology, University of Michigan, 830 North University Ave., Ann Arbor, MI 48109. Tel.: 734-647-8512; Fax: 734-647-0884; E-mail: makaabou@umich.edu.

[1] The abbreviations used are: AChE, acetylcholinesterase; AChR, acetylcholine receptor; ColQ, collagen Q; α-BTX, alpha bungarotoxin; TTX, tetrodotoxin; PBS, phosphate buffered saline; NMJs, neuromuscular junctions; DFP, diisopropylfluorophosphate; PFA, paraformaldehyde; BAPTA-AM, 1,2-bis(2-aminophenoxy)ethane-*N*,*N*,*N*′,*N*′-tetraacetic acid-acetoxymethyl ester; EPSPs, end plate postsynaptic potentials.

cence microscope, and neuromuscular junctions were viewed under a coverslip with a water immersion objective (×20 UAPO 0.7 NA Olympus BW51, Optical Analysis Corp., Nashua, NH) and digital CCD camera (Retiga EXi, Burnaby, British Columbia, Canada).

All animal usage followed methods approved by the University of Michigan Committee on the Use and Care of Animals. Mice were intubated and ventilated for the duration of the imaging sessions. For experiments in which the junction was to be re-imaged within 8 h, the animal was continuously ventilated and maintained under anesthesia by intraperitoneal doses of ketamine and xylazine every 2 h. To minimize evaporation, the muscle was bathed with lactated Ringer's containing whatever drugs were appropriate to the experiment, and a coverslip was placed over the exposed muscle. A fresh dose of drug solution was added every 2 h. For multiple time points beyond 8 h, the mouse was sutured and allowed to fully recover before the next imaging session. In some experiments, the sternomastoid muscle was stimulated by a Grass SD5 stimulator connected to two platinum wires at either side of the muscle. The stimulus pulses (3-ms bipolar pulses of 6–9 V at 10 Hz for a 1-s duration every 2 s) elicited maximal twitching and therefore action potentials in all muscle fibers.

Quantitative Fluorescence Imaging—The fluorescence intensity of labeled AChE at neuromuscular junctions was assayed by using a quantitative fluorescence imaging technique, as described by Turney and colleagues (22) with minor modification. This technique incorporates compensation for image variation that may be caused by spatial and temporal changes in the light source and camera between imaging sessions by calibrating the images with a nonfading reference standard. Image analysis was performed by using either a procedure written for IPLAB (Scanalytic, VI) or Matlab (The Mathworks, Natick, MA). Background fluorescence was approximated by selecting a boundary region around the junction and subtracting it from the original image, and the mean of the total fluorescence intensity (which corresponds to density) was measured. After saturating all pre-existing AChEs with unlabeled fasciculin2 and re-saturating newly inserted AChEs with fluorescent fasciculin2 at a later time, the mean of the total fluorescence of newly labeled AChE was expressed as the percentage of the mean of fluorescence of AChEs saturated with only Alexa 594 fasciculin2 at time 0. When average intensity is presented, it is ± S.D.

RESULTS

The Rate of Fasciculin2 Unbinding from Synapses Is Extremely Slow—The interpretation of the experiments described in this study depends on the rate of unbinding of unlabeled fasciculin2 from AChE. Based on two lines of evidence, we conclude that the rate of unbinding of unlabeled fasciculin2 is slow enough to be considered negligible over the 7-day time span we made the measurements reported in the rest of this study.

The first group of experiments was conducted on muscles dissected free of the animal, fixed, and then washed and maintained in 0.5 M glycine PBS (Fig. 1). The advantage of studying fixed tissue is that new synthesis and insertion of AChE are eliminated, so determining the rate of unbinding of fasciculin2 under these conditions is simple. We first demonstrated that neither the ability of Alexa 594-labeled fasciculin2 to interact with AChE nor the ability of Alexa 488-labeled α-bungarotoxin (α-BTX) to interact with AChR was inhibited by four different fixation conditions. In Fig. 1, muscles fixed with 2% paraformaldehyde (PFA) in PBS are shown, but similar results were obtained with 4% PFA, 8% PFA, or 2% PFA and 2% glutaraldehyde in PBS (although in the latter case autofluorescence was extremely high). Muscles fixed, washed, and labeled immediately with Alexa 594-conjugated fasciculin2 (Fig. 1, *A* and *B*) and muscles fixed, washed, and then maintained in PBS for as long as 2 months before being exposed to Alexa 594-conjugated fasciculin2 (Fig. 1, *C* and *D*) labeled with approximately equal intensity, indicating that fixation does not affect the toxin-binding sites of AChE or AChR. The AChE staining was specific, because it could be prevented by adding saturating levels of unlabeled fasciculin2 or BW284C51 (an inhibitor of AChE that competes with fasciculin2) just prior to adding Alexa 594-conjugated fasciculin2. Binding of Alexa 488 α-BTX was not affected by fasciculin2 (Fig. 1, *E–H*). The key experiment was to add unlabeled fasciculin2 shortly after washing off the fixative and then probing with Alexa 594-labeled fasciculin2 at a later time. All sites from which the unlabeled fasciculin2 had unbound and washed away should be stained with Alexa 594 fasciculin2. However, even when 2 weeks were allowed for unbinding, there was little or no detectable labeling (Fig. 1*J*).

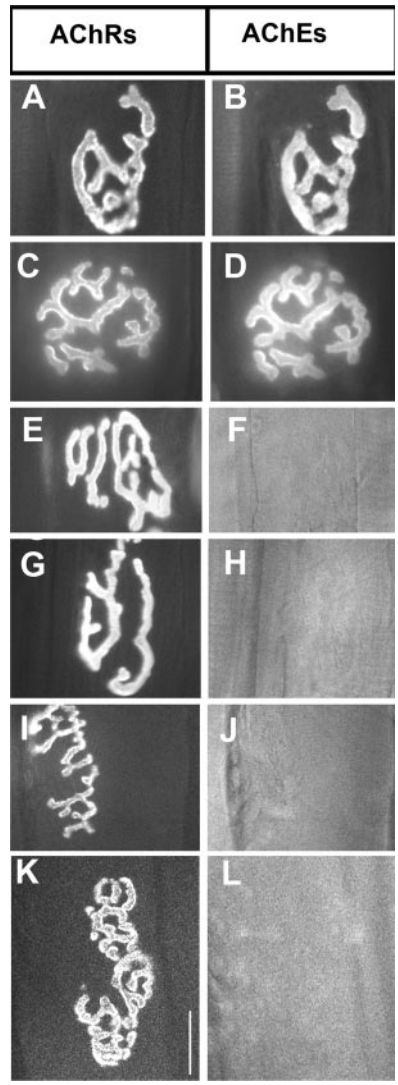

FIG. 1. **Labeling of AChE with Alexa 594 fasciculin2 after fixation of the muscle with 2% PFA in PBS demonstrates a very slow rate of fasciculin2 unbinding.** *A* and *B,* example of a superficial neuromuscular junction on a sternomastoid muscle labeled with Alexa 488 bungarotoxin and Alexa 594 fasciculin2 immediately after fixation and washed with PBS. *C* and *D,* sternomastoid muscle labeled with Alexa 488 bungarotoxin and Alexa 594 fasciculin2 2 months after fixation. *E* and *F,* sternomastoid muscle saturated with unlabeled fasciculin2 and then labeled with Alexa 488 bungarotoxin and Alexa 594 fasciculin2. *G* and *H,* sternomastoid muscle saturated with BW284C51 (an inhibitor of AChE which competes with fasciculin2) and then immediately labeled with Alexa 488 bungarotoxin and Alexa 594 fasciculin2. *I* and *J,* sternomastoid muscle saturated with unlabeled fasciculin2, washed, and labeled 2 weeks later with Alexa 488 bungarotoxin and Alexa 594 fasciculin2. *K* and *L,* sternomastoid muscle saturated with unlabeled fasciculin2 and Alexa 488 bungarotoxin and then immediately incubated with a high concentration of Alexa 594 fasciculin2 continuously for 4 days. Images were then taken at day 4. Note that there is no evidence of staining of AChEs with fluorescent fasciculin2 in *F, H* and *J*, or *L* even with high camera gain. *Scale bar* = 20 μm.

The dissociation rate we observed for fasciculin2 from AChE at synapses in fixed tissue is far slower than the published

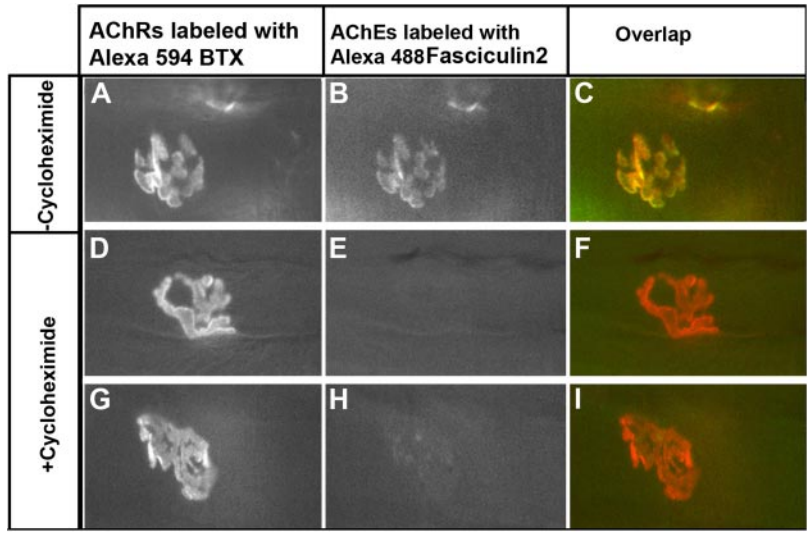

FIG. 2. **Labeling of AChE with Alexa 488 fasciculin2 in living muscle demonstrates a very slow rate of fasciculin2 unbinding.** Whole mouse diaphragm muscles were dissected from the animal and cultured for 24 h in the presence or absence of the protein synthesis inhibitor cycloheximide. Muscles were saturated with unlabeled fasciculin2 immediately after removal from the animal, washed, and then relabeled at the end of the experiment with Alexa 488 fasciculin2 and Alexa 594 α-bungarotoxin to label AChEs and AChRs, respectively. *A* and *B,* example of a neuromuscular junction of a control muscle not treated with cycloheximide, showing the presence of newly inserted AChEs. *C,* composite image of *A* and *B*. *D–I,* examples of two neuromuscular junctions of muscle incubated continuously with cycloheximide for the duration of the experiment, showing little or no staining.

unbinding rate of fasciculin2 from solubilized AChE in a test tube, which yields half-lives in the range of a few hours (12–14, 23–26). A potential explanation for the slow apparent rate of unbinding from intact synapses would be that the actual rate of unbinding is much more rapid, but that most of the time the fasciculin2 is rebound rather than diffusing away. To test this possibility, muscles were fixed with 2% PFA, washed, saturated with unlabeled fasciculin2, washed again, and then incubated continuously with a high concentration of Alexa 594 fasciculin2. Under these conditions, it is expected that any fasciculin2 that unbinds will be replaced by Alexa 594 fasciculin2, so the rate of appearance of fluorescence will provide an estimate of the rate of dissociation of unlabeled toxin uncontaminated by rebinding. When we imaged synapses that were continuously incubated in Alexa 594 fasciculin2 for 4 days, we saw little or no evidence for AChEs staining with fluorescent fasciculin2 (Fig. 1*L*).

The second group of experiments tested whether the extremely slow rate of loss of fasciculin2 was a peculiarity of fixed muscle. We placed living mouse diaphragm muscles into organ culture. Synapses were saturated with unlabeled fasciculin2, washed, and then continuously exposed for 24 h to Alexa 488-labeled fasciculin2 in the presence or absence of the protein synthesis inhibitor cycloheximide (Fig. 2). The rationale for these experiments is that in the absence of cycloheximide, the gain of fluorescence over 24 h might result from three processes as follows: 1) the loss of unlabeled fasciculin2 from pre-existing AChEs followed by rebinding of labeled fasciculin2; 2) the transfer of already synthesized AChEs that were in an intracellular compartment to the cell surface; and 3) the accumulation of newly synthesized AChEs on the surface. Cycloheximide will eliminate or dramatically affect this third possible pathway. In the absence of cycloheximide (Fig. 2, *A–C*), there was intensive synaptic labeling with Alexa 488-labeled fasciculin2. On average, the intensity was 18% that of control labeled with only Alexa 488-fasciculin2 (that had not been exposed to unlabeled fasciculin2). After 24 h in the presence of cycloheximide, the Alexa 488 fluorescence was barely detectable (Fig. 2, *D–I*). The average intensity of the Alexa 488 fasciculin2-labeled synapses from cycloheximide-treated muscles was 1–3% of noncycloheximide-treated muscle. If this entire signal was because of fasciculin2 dissociation that followed an exponential time course, this would correspond to a half-life of about 35 days. Because the transfer of pre-existing AChEs to the surface also contributes to this signal, the actual half-life for dissociation is even longer than this. Thus, these experiments were sufficient to conclude that the loss of unlabeled fasciculin2 from AChE in living muscle must be very slow, just as was the case for fixed muscle.

AChE Insertion at the Neuromuscular Junction in Living Mice following a Single Saturating Dose of Fasciculin2—To determine the number of new AChEs inserted into the neuromuscular junctions of living animals over time, the sternomastoid muscle of six mice at each data point was bathed with unlabeled fasciculin2 (7 μg/ml, 2.5 h) to saturate all pre-existing AChEs. We confirmed that all AChEs were saturated by adding a fluorescently conjugated Alexa 594 fasciculin2 (7 μg/ml, 10 min) and demonstrating an absence of red fluorescence. Because the rate of unbinding of unlabeled fasciculin2 is undetectably slow (see above), any red fluorescence detected after re-labeling the muscle with Alexa 594 fasciculin2 at a later time must come from the binding of fasciculin2 to newly inserted AChE. The new AChE will include both newly synthesized molecules and AChE that was already present but not on the surface. The number of AChEs inserted after initial saturation of the NMJ with unlabeled fasciculin2 was expressed as a percentage of the fluorescence present when control neuromuscular junctions were saturated with Alexa 594 fasciculin2 and immediately imaged (Fig. 3, *A* and *B*). After saturating all pre-existing AChEs with unlabeled fasciculin2 and re-saturating newly inserted AChEs with Alexa 594 fasciculin2 4 h later, we found that the recovery of fluorescence was ~6 ± 3% (n = 50) of the total fluorescence of AChEs saturated with only Alexa 594 fasciculin2 (Fig. 3, *A* and *B*). At 8 and 24 h and 3 and 7 days after saturating all pre-existing AChEs with unlabeled fasciculin2, the recovery of fluorescence intensity was, respectively, 11 ± 3% (n = 40), 20 ± 3% (n = 15), 35 ± 5% (n = 30), and 65 ± 9% (n = 25) of total fluorescence at synapses saturated only with Alexa 594 fasciculin2 (Fig. 3, *A* and *B*). This AChE recovery corresponds to an initial rate of about 2% per h ($t_{1/2}$ ~46 h), which slowed by 7 days to 0.7% per h ($t_{1/2}$ ~7 days). Our results showing that AChE insertion is initially rapid differ dramatically from previous reports claiming that the insertion of AChE does not occur until 3–7 days after initial blockade with DFP, an organophosphate esterase inhibitor, and that the rate of insertion is very slow at all times (27) (see "Discussion").

AChE Insertion into the Neuromuscular Junction Depends on Muscle Postsynaptic Activity—Because many processes in skeletal muscle are regulated by synaptic activity, we carried out three types of experiments to test the role of activity in regulating the rate of appearance of new AChE. All three approaches used toxins that decrease muscle activity by different mechanisms. α-BTX (10 μg/ml) blocks nAChRs, and so a

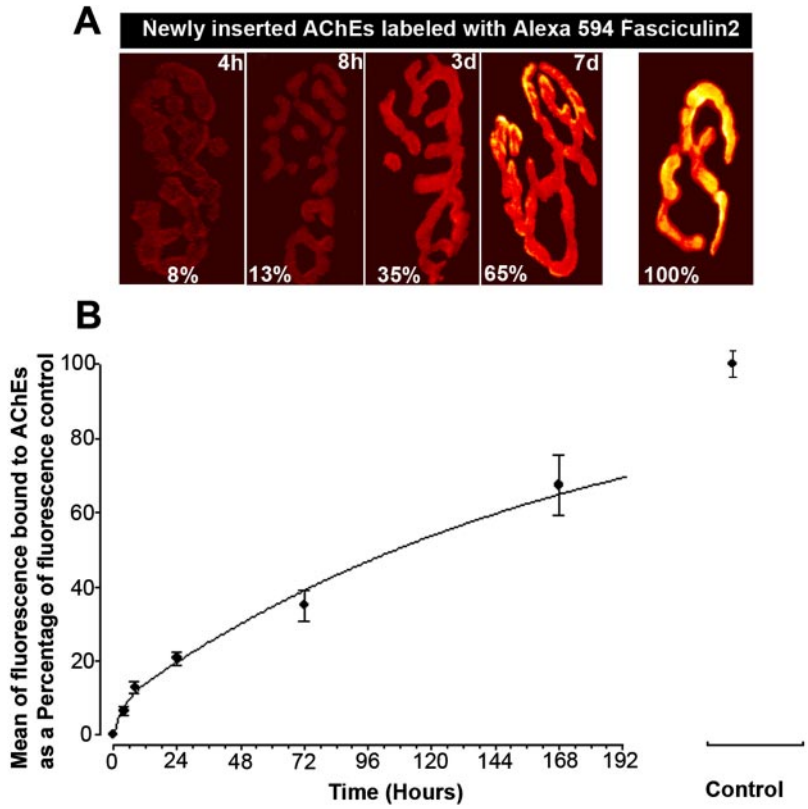

FIG. 3. **Insertion of new AChE over time.** From 4 h to 7 days after initial saturation of pre-existing AChEs with unlabeled fasciculin2, groups of mice were re-anesthetized, and newly inserted AChEs were labeled with Alexa 594 fasciculin2. Superficial synapses were imaged, and their fluorescence intensity was assayed. *A,* examples of superficial neuromuscular junctions saturated with unlabeled fasciculin2 at time 0 and then treated with a saturating concentration of Alexa 594 fasciculin2 and imaged at 4, 8, 72, and 168 h later. These pseudocolor images provide a linear representation of the density of AChEs (*white-yellow*, high density; *red-black*, low density). The dim appearance of AChE labeling at earlier time points (4 and 8 h) permitted all panels to be shown on the same intensity scale. The *numbers* indicate the average fluorescence intensity of these junctions. *B,* quantification of neuromuscular AChE insertion from 4 to 168 h. Each data point represents the mean and S.D. of the total fluorescence of individual superficial junctions labeled with Alexa 594 fasciculin2, converted to percent of fluorescence intensity of synapses immediately labeled with Alexa 594 fasciculin2.

saturating dose directly eliminates evoked and miniature end plate postsynaptic potentials (EPSPs) and indirectly eliminates action potentials in the muscle. TTX (1 μg/ml) blocks voltage-gated sodium channels on both axons and on muscle fibers, and so also indirectly blocks evoked EPSPs, while leaving miniature EPSPs intact. μ-Conotoxin GIIIB (2 μM) selectively blocks voltage-gated sodium channels on muscle fibers, while sparing those on axons, leaving neuronal action potentials and both evoked and miniature EPSPs unchanged while blocking muscle action potentials (28).

The experimental paradigm used to test the effect of exogenous agents on AChE insertion was to apply a saturating dose of unlabeled fasciculin2 (7 μg/ml, 2.5 h) to the sternomastoid muscle followed by a second dose of Alexa 594 fasciculin2 (7 μg/ml, 10–20 min), to be sure that all synapses were saturated with unlabeled fasciculin2, and then to continuously bathe the muscle with a toxin for 8 h (with reapplication every 2 h to make sure that the agent was present continuously). At the end of this period, Alexa 594 fasciculin2 was applied at a saturating dose to label all AChEs that had been inserted over that time. These treatments required that animals be continuously ventilated and could not be carried beyond 8 h because of mortality. The fluorescence of synapses in toxin-treated animals was approximately half the fluorescence of synapses in control animals labeled similarly but not treated with any toxin (α-BTX 46 ± 7% (n = 40); TTX 50 ± 8% (n = 25); and μ-conotoxin GIIIB 46 ± 8% (n = 35); Fig. 4, *A–F*). Thus new AChE can appear in the absence of spike activity in the muscle at a basal rate, but the rate of AChE appearance was doubled when muscle action potentials were not blocked. Neither presynaptic spikes nor synaptic potentials were able to increase the appearance of new AChE above the basal level if muscle action potentials were absent.

Muscle Postsynaptic Activity Restores AChE Insertion—As a final test of the role of muscle spike activity on AChE insertion, the sternomastoid muscle was first bathed with unlabeled fasciculin2 to saturate all pre-existing AChEs, and postsynaptic muscle activity was eliminated by blocking synaptic transmission with a high dose of α-bungarotoxin (10 μg/ml), and then action potentials were directly elicited by placing stimulating electrodes at either end of the muscle (3-ms bipolar pulses of 6–9 V at 10 Hz for 1-s duration every 2 s for the entire 8-h period). During the duration of this experiment, the mouse was intubated and ventilated to prevent asphyxia. We found that the level of expression of AChE in these muscles (112 ± 16%, n = 40) was approximately double the level found in muscles treated with α-BTX alone and was not significantly different from untreated control muscles (Fig. 5, *A* and *B*). This result indicates that muscle action potentials are necessary and sufficient to maintain normal levels of AChE insertion.

Intracellular Calcium Levels Are Critical for AChE Insertion—Muscle contraction is the consequence of an elevation of intracellular calcium. It therefore seemed possible that the molecular mechanism by which muscle activity modulates AChE insertion also requires an elevation of intracellular calcium. To test this hypothesis, four different types of experiments were carried out.

One way for calcium to become elevated is by entering the cell through voltage-activated channels in the plasma membrane. In innervated adult mouse skeletal muscle, only one type of voltage-gated calcium channel (the L-type channel that is slowly activated and inactivated by depolarization and can be blocked by dihydropyridines and verapamil) has been described (29–32). To determine the potential role of Ca^{2+} flux through this channel on AChE insertion rates, the sternomastoid muscle was incubated with unlabeled fasciculin2 to saturate all pre-existing AChEs and then electrically stimulated in the presence of a high dose of unlabeled bungarotoxin (to block calcium entry through AChRs) and verapamil (50 μM) (to block calcium entry through voltage-gated L-type Ca^{2+} channels) for the duration of the experiment. Eight hours later, newly inserted AChEs were labeled with Alexa 594 fasciculin2, and their fluorescence intensity was measured. We found that the fluorescence of newly inserted AChE was only 45 ± 8% (n = 23) of the total fluorescence of control muscle

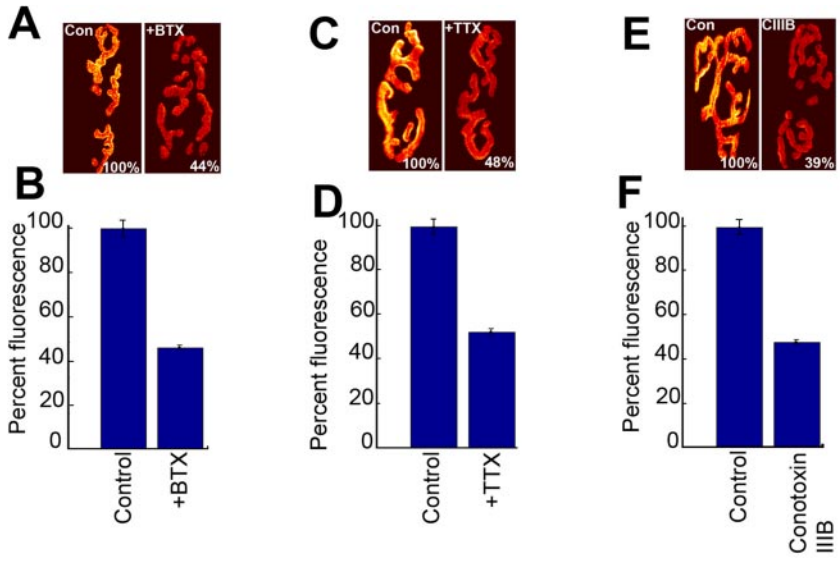

FIG. 4. **Postsynaptic activity blockade decreased AChE insertion into synapses *in vivo*.** *A,* example of a neuromuscular junction that was saturated at time 0 with unlabeled fasciculin2 and saturated again 8 h later with Alexa 594 fasciculin2 (*1st panel*), and a junction labeled in the same way but chronically blocked with unlabeled bungarotoxin (*2nd panel*). *Con*, control. *B, histogram* summarizing the amount of synaptic AChE insertion during chronic muscle activity blockade with α-BTX and or at unblocked synapses at 8 h. *C,* example of a control neuromuscular junction (*1st panel*) and an NMJ in the continuous presence of TTX for 8 h (*2nd panel*). *D, histogram* summarizing the amount of new AChE insertion in control and TTX-treated muscles at 8 h. *E,* example of a control NMJ (*1st panel*) and an NMJ in which muscle sodium channels were chronically blocked with μ-conotoxin IIIB (*2nd panel*). *F, histogram* summarizing insertion of new AChE from many synapses of blocked and unblocked control muscle at 8 h.

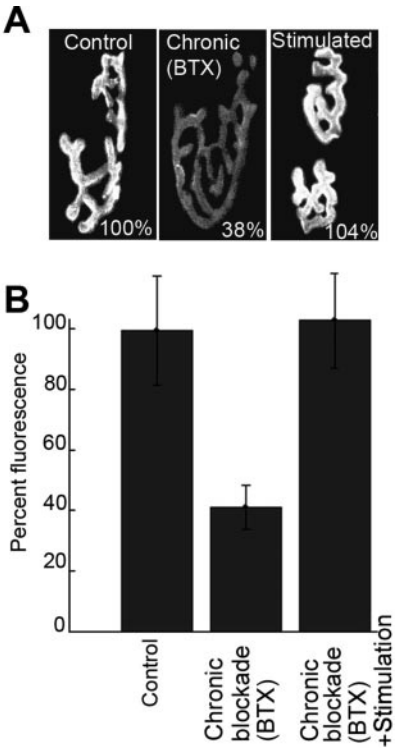

FIG. 5. **Direct stimulation of blocked muscle restored AChE insertion to control levels.** *A,* neuromuscular junctions were incubated with unlabeled fasciculin2 to saturate all pre-existing AChEs, and then postsynaptic activity was chronically blocked with unlabeled bungarotoxin while the muscle was stimulated for 8 h. To determine the amount of AChE insertion, Alexa 594 fasciculin2 was added at 8 h. AChE insertion was greatly diminished at chronically blocked junctions (*2nd panel*). However, in muscles that were directly stimulated during bungarotoxin blockade, the insertion rate was comparable with control (*3rd panel*). *B, histogram* shows the insertion of new AChEs at control, BTX-blocked, and BTX-stimulated muscle at 8 h.

synapses labeled after 8 h with Alexa 594 fasciculin2 (Fig. 6, *A* and *C*). However, in unstimulated muscle this drug had little effect on AChE insertion. These results suggest that calcium entry through voltage-dependent calcium channels is involved in AChE insertion.

A second mechanism for elevating intracellular free calcium is Ca^{2+} release from the sarcoplasmic reticulum. To investigate whether the release of intracellular calcium from the sarcoplasmic reticulum in the absence of muscle activity can modulate AChE insertion, muscle postsynaptic activity was chronically blocked with unlabeled α-BTX in the presence of ryanodine, a plant alkaloid known to release calcium from the sarcoplasmic reticulum (33–35). Treatment with 0.3 μM ryanodine, a concentration known to tonically elevate intracellular free calcium (36), resulted in AChE insertion levels comparable with those of control muscles (115 $\pm$ 18%, n = 38) and double those in muscles treated with α-BTX alone, indicating that directly releasing calcium from intracellular stores can bypass the need for spike activity to elevate AChE insertion (Fig. 6, *B* and *C*). Verapamil was unable to inhibit the effect of 0.3 μM ryanodine, arguing that the calcium flux through L-type channels is not required to replenish the intracellular calcium stores in the sarcoplasmic reticulum. In contrast, treatment with 100 μM ryanodine, which transiently elevates intracellular free calcium but then leaves the stores depleted for many hours (36), resulted in only basal levels of AChE insertion or Ca^{2+} concentration (data not shown).

A third test of the involvement of intracellular free calcium in AChE insertion was to bypass all normal cellular pathways and to elevate intracellular free calcium directly by adding the Ca^{2+} ionophore A23187 (3 μM). Treatment of α-BTX-blocked muscles with A23187 elicited an increase in the expression of AChE to about double the base-line value (100 $\pm$ 7%, n = 25) (Fig. 6, *D* and *F*), as would be expected if a rise in intracellular free calcium plays a role in AChE insertion.

Finally, we examined the effect of adding an exogenous calcium buffer into the muscle cells, with the expectation that this might attenuate the spike-induced increase in intracellular free calcium. Chronic exposure to BAPTA-AM (500 μM) for 8 h decreased the level of AChE insertion to 17 $\pm$ 5% (n = 20) (Fig. 6, *E* and *F*) of control fluorescence, significantly below the basal level of about 50% seen in all other treatments that blocked activity. This effect was specific, as the treatment with Mag-Fura2-AM, which would produce the same waste product as BAPTA-AM but has a much lower affinity for calcium than BAPTA and thus should be incapable of chelating physiological levels of calcium, had no effect on AChE insertion. An implication of the BAPTA result is that the basal level of intracellular free calcium normally found in resting cells may be sufficient to account for much of the basal level of AChE insertion.

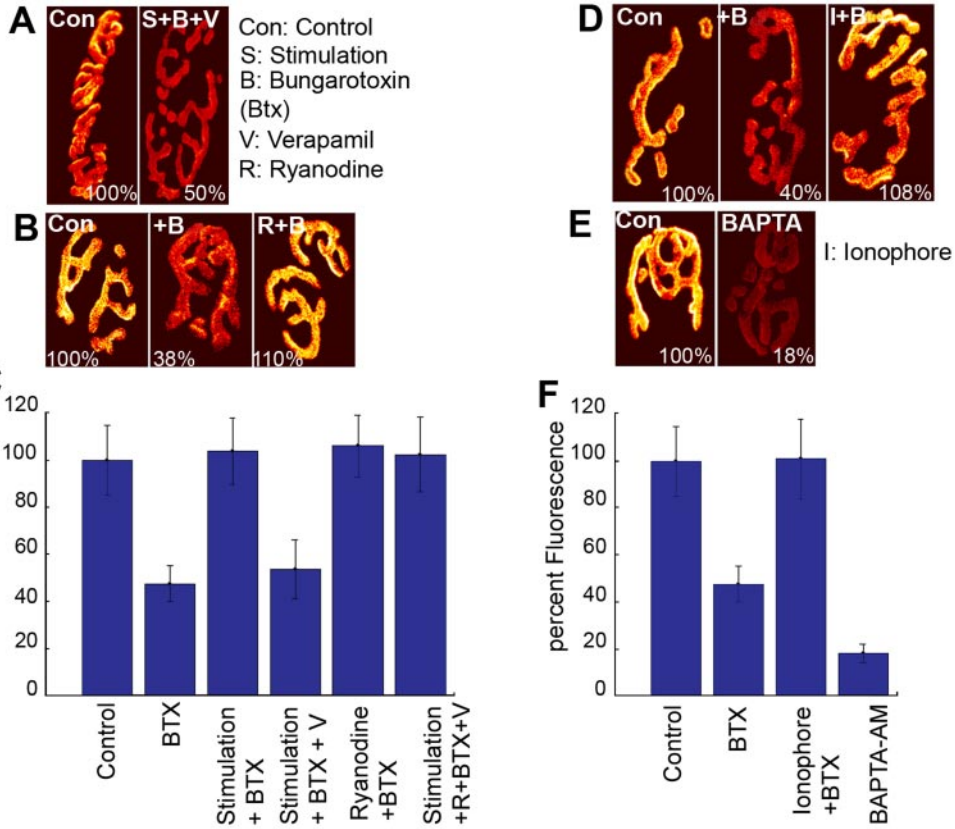

FIG. 6. **The AChE insertion rate is mediated by calcium influxes through voltage-gated calcium channels as well as from the sarcoplasmic reticulum.** Sternomastoid muscles were bathed with unlabeled fasciculin2 to saturate all pre-existing AChEs and re-labeled at 8 h with Alexa 594 fasciculin2 under different calcium manipulation conditions. *A,* example of control NMJ and neuromuscular junction stimulated for 8 h in the presence of unlabeled bungarotoxin and verapamil. *B,* example of control, BTX-blocked, and BTX-blocked neuromuscular junctions incubated with ryanodine. *C, histogram* represents the insertion of AChE in control, BTX-blocked, BTX-stimulated, and BTX-stimulated verapamil and ryanodine. *D,* example of a control NMJ (*1st panel*), an NMJ chronically blocked with BTX (*2nd panel*), and an NMJ chronically blocked with BTX in the presence of ionophore A12387 (*3rd panel*). *E,* example of a control NMJ (*1st panel*) and an NMJ treated with the membrane-permeable calcium chelator BAPTA-AM. *F, histogram* represents AChE insertion detected with Alexa 594 fasciculin2 in control, chronic BTX-blocked, and BTX-blocked synapses in presence of ionophore A12387.

DISCUSSION

We have examined AChE insertion in living synapses with a new experimental approach, and we have demonstrated that the rate of insertion of junctional AChE is dependent upon activity. Within the first few hours after a single saturating dose of unlabeled fasciculin2 (to make all pre-existing AChE invisible), the appearance of new AChE was readily detected with Alexa-labeled fasciculin2. When postsynaptic spike activity was blocked in a variety of ways, the rate of AChE insertion was dramatically slowed. Direct stimulation of the muscle while synaptic transmission was blocked restored the insertion rate to its normal level. Elevation of intracellular free calcium in the muscle cells was shown to be an essential step in achieving the maximum rate of AChE delivery. Under our standard experimental paradigm, a significant proportion of the new AChE (about 50% of control) still appeared when muscle spiking was inhibited. Thus, there is activity-dependent and activity-independent delivery of AChE. One potential explanation is that there are two separate molecular mechanisms for regulating AChE delivery to the synaptic cleft. However, these results could also be explained by a single molecular mechanism that is calcium-dependent, if the basal level of intracellular free calcium is sufficient to allow the delivery of AChE to the synaptic cleft at about half of its maximal rate. The ability of the calcium chelator BAPTA to decrease the AChE delivery rate much more than inhibition of muscle spike activity alone is consistent with the latter possibility.

The rapid appearance of new Alexa fasciculin2-binding sites could not be explained by the unbinding of fasciculin2 from pre-existing AChE. In addition to the two lines of evidence that fasciculin2 unbinding was extremely slow as presented under "Results," a third line of experiments also led to the same conclusion.[2] When living synapses or fixed synapses were labeled with Alexa 594 fasciculin2 at day 0 and the intensity of fluorescence was measured at a later time, there was a slow but readily detectable loss of fluorescence over time, with about 10% loss over 7 days. As the converse experiment we performed in the work reported here showed no detectable unbinding of unlabeled fasciculin2 over 7 days, we concluded that the rate of unbinding for Alexa-conjugated fasciculin2 is more rapid than the rate of unbinding of unlabeled fasciculin2. It was based on these experiments that we developed the protocol used here to study the insertion of new AChE. A final reason for concluding that the gain of fluorescence over time represents insertion of new AChE and not unbinding form existing sites is that the rate of increase in fluorescence intensity was regulated by the blockade of postsynaptic activity, direct muscle stimulation, and calcium manipulations. An unexpectedly rapid rate of dissociation of fasciculin2 from AChE would not explain any of these results.

The half-life of fasciculin2 unbinding from AChE that we estimate at synapses in fixed and living mouse muscle is in excess of 35 days. This is far slower that the half-life of 1–6 h

[2] E. Krejci and M. Akaaboune, unpublished observations.

(14, 15, 37) that has been reported by others for fasciculin2 unbinding from solubilized AChE in a test tube. It is worth noting that the unbinding of fasciculin2 from AChE is not the only synaptic interaction that shows great differences between the *in vitro* and *in vivo* cases. Binding of α-bungarotoxin to solubilized AChR in test tubes also has a much shorter half-life (30–60 h) (38, 39) compared with the half-life found in live tissue (10–14 days) or fixed tissue (~ months) (21, 40).

What might account for the vast differences in dissociation rate between the *in vivo* and *in vitro* situations? It is unlikely to be a species difference, because the measurements of the k_{off} value of fasciculin2 *in vitro* were performed on AChE from several sources, including recombinant mouse AChE (24–26, 37), and we studied AChE at mouse synapses. The assays used in the two types of studies were very different measurements of recovery of AChE activity in the *in vitro* studies and fluorescence intensity in our studies, but there is no reason to suspect that one assay reports more accurately than the other. Another possibility was that because of the very high concentration of AChE at synapses (AChE concentration in the synaptic cleft is in the range of 0.2 mM), a single fasciculin2 molecule might bind and rebind many times before escaping the synapse, thus producing an apparent unbinding rate much slower than the actual rate of dissociation of the molecular complex. However, the experiments presented in Fig. 2 suggest that this is not the case. A potential explanation for the difference in results is that AChE was in very different states in the two types of experiments. For example, the *in vitro* studies were of soluble AChE produced in cell lines or erythrocytes (15), and it is possible that the pattern of glycosylation or another post-translational modification differs between these tissues and skeletal muscle. Perhaps a more likely explanation is that the *in vitro* measurements were made on soluble, monomeric AChE, whereas at the synapse AChE is organized into tetramers by ColQ. Thus it seems possible that when AChEs are extracted from their native milieu, they are altered in a way that greatly decreases their affinity for fasciculin2. It is clear that ColQ changes some molecular properties of esterase, as human AChE produced in stably transfected cell lines is degraded faster when it lacks a ColQ-derived proline-rich attachment domain (41, 42). These results suggest that ColQ may be a key control point for modulating the conformation of AChE in the synaptic cleft, and it would be interesting to explore whether the catalytic activity of this enzyme differs depending on whether or not it is bound to ColQ.

The rapid time course of AChE insertion demonstrated by our work also departs significantly from previous findings that suggested that the rate of appearance of new AChE is extremely slow ($t_{1/2}$ of ~20 days) (43) and that AChE insertion is delayed between 3 and 7 days after inhibition of esterase function alone (44). This delay was attributed to damage to the muscle from excess ion fluxes when the esterase was nonfunctional (45, 46). In these experiments, inhibition of AChE was always followed by nerve stimulation to monitor muscle contraction and to ensure that all AChEs were inhibited with DFP. By doing so, a significant amount of acetylcholine must have accumulated in the synaptic cleft. This would lead to an increase in the amount of time that AChR spent in the open state and therefore an increased calcium influx that could generate a local necrosis in the postsynaptic site. In contrast, in the experiments in which we simultaneously added fasciculin2 and permanently blocked AChRs with α-bungarotoxin, the amount of "new" AChE insertion was significantly decreased compared with synapses labeled with fasciculin2 alone or incubated after a one-time bungarotoxin blockade. The differences in AChE insertion rate between our results and previous work could be because of several factors. First, the previous studies used the nonspecific AChE inhibitor DFP as a probe for AChE. Because DFP is lipid-soluble and can interact with a variety of esterases in addition to AChE, its use is problematic. For example, it is possible that DFP inhibits intracellular pools of AChE and other esterases that may be involved in the secretion of AChE into the basal lamina, thus affecting its recovery (27, 47). It is also possible that inactivation of extra- and intracellular Seiren hydrolases by DFP may alter their involvement in the remodeling of extracellular matrix proteins. DFP labeling also results in high background, which makes the detection of low synaptic AChE density impossible to study (48, 49). Finally, the DFP-labeling procedure *per se*, which involves a complex sequence of inhibition and reactivation steps that allow detection of DFP sites by electron microscopy using a very long exposure time (months), could be potential sources for a lack of sensitivity (48, 49).

Our results reporting rapid, activity-dependent AChE insertion are consistent with a large number of other properties of AChE expression that are know to be regulated by activity. These include the localization of AChE at the synapse and its decrease from extra-synaptic sites (50–52). However, one complication of our experimental paradigm is that fasciculin2 completely inhibits AChE function (16), so our initial application of unlabeled fasciculin2 could produce an alteration in synaptic transmission as a consequence of the failure to rapidly degrade acetylcholine. In the initial period when AChE activity is completely blocked, the physiological effect will depend critically upon the frequency and pattern of spike activity in the motor neurons. If the spike frequency is sufficiently high, it will chronically elevate acetylcholine in the cleft, and would be expected to produce an inhibition of muscle spiking as a consequence of either AChR desensitization or tonic depolarization of the muscle to a level that inactivates voltage-gated sodium channels. However, if the spike frequency is low, diffusion alone might be sufficient to clear the cleft of acetylcholine between spikes, and the effect of inhibiting AChE would be to produce larger synaptic currents with each spike, with no interruption of spiking in the muscle. Given our evidence that the level of intracellular free calcium controls the rate of AChE insertion, we speculate that the net effect of transient inhibition of AChE is to elevate intracellular free calcium, and that this is the signal that transiently enhances the rate of AChE insertion.

The work presented here suggests that the regulation of AChR and AChE dynamics at synapses might share some of the same cellular and molecular control mechanisms. For example, synaptic activity is critical for increasing the delivery and insertion of AChR at end plates and decreasing insertion into the extra-synaptic pools (3, 4). The role we postulate for intracellular calcium in regulating the delivery of AChE is also similar to the role this signal is thought to play in regulating several aspects of AChR dynamics (29, 53). For example it has been shown that a decrease of AChR synthesis is associated with decreased levels of intracellular calcium (54) through unknown mechanisms that can also regulate again-induced receptor clustering (55, 56). Also intracellular calcium was found to increase the synthesis of collagen-tailed AChE in cell culture (57). Although these regulations may both involve intracellular calcium, it is possible that AChE and AChR are affected in opposite manners. The interpretation of some experiments involving AChR and calcium is complicated by the fact that the removal of extracellular calcium has also been shown to destabilize AChR clusters (58–60). The overall pattern of results, however, suggests that many aspects of AChR and AChE dynamics are regulated by the same factors, which would be an

efficient way to ensure that the appropriate balance of these two essential synaptic signaling molecules is maintained.

Acknowledgments—We thank Raffia Ameziane, Emile Bruneau, and John Kuwada and members of our laboratories for helpful discussions about this work.

REFERENCES

1. Katz, B., and Miledi, R. (1973) *J. Physiol.* (*Lond.*) **231,** 549–574
2. Soreq, H., and Seidman, S. (2001) *Nat. Rev. Neurosci.* **2,** 294–302
3. Sanes, J. R., and Lichtman, J. W. (1999) *Annu. Rev. Neurosci.* **22,** 389–442
4. Sanes, J. R., and Lichtman, J. W. (2001) *Nat. Rev. Neurosci.* **2,** 791–805
5. Deprez, P., Inestrosa, N. C., and Krejci, E. (2003) *J. Biol. Chem.* **278,** 23233–23242
6. Rotundo, R. L., Rossi, S. G., and Anglister, L. (1997) *J. Cell Biol.* **136,** 367–374
7. Cartaud, A., Strochlic, L., Guerra, M., Blanchard, B., Lambergeon, M., Krejci, E., Cartaud, J., and Legay, C. (2004) *J. Cell Biol.* **165,** 505–515
8. Ohno, K., Brengman, J., Tsujino, A., and Engel, A. G. (1998) *Proc. Natl. Acad. Sci. U. S. A.* **95,** 9654–9659
9. Feng, G., Krejci, E., Molgo, J., Cunningham, J. M., Massoulié, J., and Sanes, J. R. (1999) *J. Cell Biol.* **144,** 1349–1360
10. Arikawa-Hirasawa, E., Rossi, S. G., Rotundo, R. L., and Yamada, Y. (2002) *Nat. Neurosci.* **5,** 119–123
11. Karlsson, E., Mbugua, P. M., and Rodriguez-Ithurralde, D. (1984) *J. Physiol.* (*Paris*) **79,** 232–240
12. Harel, M., Kleywegt, G. J., Ravelli, R. B., Silman, I., and Sussman, J. L. (1995) *Structure* (*Lond.*) **3,** 1355–1366
13. Bourne, Y., Taylor, P., and Marchot, P. (1995) *Cell* **83,** 503–512
14. Marchot, P., Bourne, Y., Prowse, C. N., Bougis, P. E., and Taylor, P. (1998) *Toxicon* **36,** 1613–1622
15. Eastman, J., Wilson, E. J., Cervenansky, C., and Rosenberry, T. L. (1995) *J. Biol. Chem.* **270,** 19694–19701
16. Rosenberry, T. L., Rabl, C. R., and Neumann, E. (1996) *Biochemistry* **35,** 685–690
17. Anglister, L., Eichler, J., Szabo, M., Haesaert, B., and Salpeter, M. M. (1998) *J. Neurosci. Methods* **81,** 63–71
18. Peng, H. B., Xie, H., Rossi, S. G., and Rotundo, R. L. (1999) *J. Cell Biol.* **145,** 911–921
19. van Mier, P., and Lichtman, J. W. (1994) *J. Neurosci.* **14,** 5672–5686
20. Lichtman, J. W., Magrassi, L., and Purves, D. (1987) *J. Neurosci.* **7,** 1215–1222
21. Akaaboune, M., Culican, S. M., Turney, S. G., and Lichtman, J. W. (1999) *Science* **286,** 503–507
22. Turney, S. G., Culican, S. M., and Lichtman, J. W. (1996) *J. Neurosci. Methods* **64,** 199–208
23. Marchot, P., Khelif, A., Ji, Y. H., Mansuelle, P., and Bougis, P. E. (1993) *J. Biol. Chem.* **268,** 12458–12467
24. Radic, Z., Duran, R., Vellom, D. C., Li, Y., Cervenansky, C., and Taylor, P. (1994) *J. Biol. Chem.* **269,** 11233–11239
25. Radic, Z., Quinn, D. M., Vellom, D. C., Camp, S., and Taylor, P. (1995) *J. Biol. Chem.* **270,** 20391–20399
26. Radic, Z., Kirchhoff, P. D., Quinn, D. M., McCammon, J. A., and Taylor, P. (1997) *J. Biol. Chem.* **272,** 23265–23277
27. Rogers, A. W., Darzynkiewicz, Z., Salpeter, M. M., Ostrowski, K., and Barnard, E. A. (1969) *J. Cell Biol.* **41,** 665–685
28. Cruz, L. J., Gray, W. R., Olivera, B. M., Zeikus, R. D., Kerr, L., Yoshikami, D., and Moczydlowski, E. (1985) *J. Biol. Chem.* **260,** 9280–9288
29. Rotzler, S., Schramek, H., and Brenner, H. R. (1991) *Nature* **349,** 337–339
30. McCleskey, E. W. (1985) *J. Physiol.* (*Lond.*) **361,** 231–249
31. Beam, K. G., and Knudson, C. M. (1988) *J. Gen. Physiol.* **91,** 781–798
32. Cognard, C., Lazdunski, M., and Romey, G. (1986) *Proc. Natl. Acad. Sci. U. S. A.* **83,** 517–521
33. Fairhurst, A. S. (1974) *Am. J. Physiol.* **227,** 1124–1131
34. Fairhurst, A. S. (1973) *Biochem. Pharmacol.* **22,** 2815–2827
35. Jenden, D. J., and Fairhurst, A. S. (1969) *Pharmacol. Rev.* **21,** 1–25
36. Meissner, G. (1986) *J. Biol. Chem.* **261,** 6300–6306
37. Radic, Z., and Taylor, P. (2001) *J. Biol. Chem.* **276,** 4622–4633
38. Darveniza, P., Morgan-Hughes, J. A., and Thompson, E. J. (1979) *Biochem. J.* **181,** 545–557
39. Betz, H. (1981) *Eur. J. Biochem.* **117,** 131–139
40. Andreose, J. S., Xu, R., Lomo, T., Salpeter, M. M., and Fumagalli, G. (1993) *J. Neurosci.* **13,** 3433–3438
41. Chitlaru, T., Kronman, C., Velan, B., and Shafferman, A. (2001) *Biochem. J.* **354,** 613–625
42. Chitlaru, T., Kronman, C., Velan, B., and Shafferman, A. (2002) *Biochem. J.* **363,** 619–631
43. Kasprzak, H., and Salpeter, M. M. (1985) *J. Neurosci.* **5,** 951–955
44. Salpeter, M. M., Kasprzak, H., Feng, H., and Fertuck, H. (1979) *J. Neurocytol.* **8,** 95–115
45. Leonard, J. P., and Salpeter, M. M. (1979) *J. Cell Biol.* **82,** 811–819
46. Wecker, L., Mrak, R. E., and Dettbarn, W. D. (1986) *Fundam. Appl. Toxicol.* **6,** 172–174
47. Barnard, E. A., Wieckowski, J., and Chiu, T. H. (1971) *Nature* **234,** 207–209
48. Salpeter, M. M., Plattner, H., and Rogers, A. W. (1972) *J. Histochem. Cytochem.* **20,** 1059–1068
49. Anglister, L., Stiles, J. R., and Salpeter, M. M. (1994) *Neuron* **12,** 783–794
50. Lomo, T., and Slater, C. R. (1980) *J. Physiol.* (*Lond.*) **303,** 173–189
51. Weinberg, C. B., and Hall, Z. W. (1979) *Dev. Biol.* **68,** 631–635
52. Rubin, L. L., Schuetze, S. M., Weill, C. L., and Fischbach, G. D. (1980) *Nature* **283,** 264–267
53. O'Malley, J. P., Moore, C. T., and Salpeter, M. M. (1997) *J. Cell Biol.* **138,** 159–165
54. McManaman, J. L., Blosser, J. C., and Appel, S. H. (1981) *J. Neurosci.* **1,** 771–776
55. Borges, L. S., Lee, Y., and Ferns, M. (2002) *J. Neurobiol.* **50,** 69–79
56. Megeath, L. J., and Fallon, J. R. (1998) *J. Neurosci.* **18,** 672–678
57. De La Porte, S., Vigny, M., Massoulie, J., and Koenig, J. (1984) *Dev. Biol.* **106,** 450–456
58. Wallace, B. G. (1988) *J. Cell Biol.* **107,** 267–278
59. Caroni, P., Rotzler, S., Britt, J. C., and Brenner, H. R. (1993) *J. Neurosci.* **13,** 1315–1325
60. Dmytrenko, G. M., and Bloch, R. J. (1993) *Exp. Cell Res.* **206,** 323–334